Article

NMR Assignment Methods for the Aromatic Ring Resonances of Phenylalanine and Tyrosine Residues in Proteins

Takuya Torizawa, Akira Mei Ono, Tsutomu Terauchi, and Masatsune Kainosho

J. Am. Chem. Soc., **2005**, 127 (36), 12620-12626• DOI: 10.1021/ja051386m • Publication Date (Web): 20 August 2005

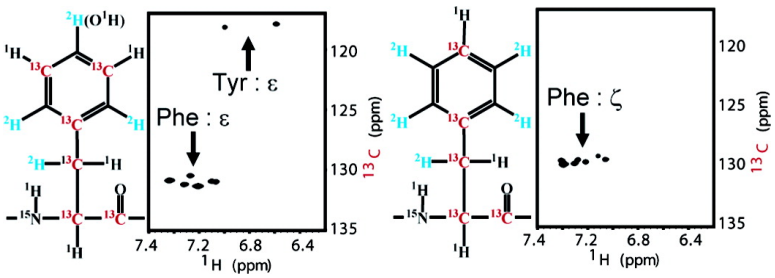

More About This Article

Additional resources and features associated with this article are available within the HTML version:

- Supporting Information
- Links to the 4 articles that cite this article, as of the time of this article download
- Access to high resolution figures
- Links to articles and content related to this article
- Copyright permission to reproduce figures and/or text from this article

View the Full Text HTML

J|A|C|S
ARTICLES
Published on Web 08/20/2005

NMR Assignment Methods for the Aromatic Ring Resonances of Phenylalanine and Tyrosine Residues in Proteins

Takuya Torizawa,† Akira Mei Ono,† Tsutomu Terauchi,† and Masatsune Kainosho*,†,‡

CREST-JST and Graduate School of Science, Tokyo Metropolitan University, 1-1 Minami-ohsawa, Hachioji, 192-0397, Japan

Received March 4, 2005; E-mail: kainosho@nmr.chem.metro-u.ac.jp

Abstract: The unambiguous assignment of the aromatic ring resonances in proteins has been severely hampered by the inherently poor sensitivities of the currently available methodologies developed for uniformly $^{13}C/^{15}N$-labeled proteins. Especially, the small chemical shift differences between aromatic ring carbons and protons for phenylalanine residues in proteins have prevented the selective observation and unambiguous assignment of each signal. We have solved all of the difficulties due to the tightly coupled spin systems by preparing regio-/stereoselectively $^{13}C/^{2}H/^{15}N$-labeled phenylalanine (Phe) and tyrosine (Tyr) to avoid the presence of directly connected $^{13}C-^{1}H$ pairs in the aromatic rings. The superiority of the new labeling schemes for the assignment of aromatic ring signals is clearly demonstrated for a 17 kDa calcium binding protein, calmodulin.

Introduction

As aromatic amino acid residues are often located in the hydrophobic core regions of proteins, structural data, such as the nuclear Overhauser effect (NOE) cross-peaks associated with the ring protons, are crucial for determining protein structures by NMR.[1−4] However, the insufficient chemical shift dispersions of the ^{1}H and/or ^{13}C resonances of the aromatic ring resonances have frequently made the detection of the individual resonances of the aromatic ring very difficult or even impossible for conventional, uniformly $^{13}C,^{15}N$-labeled proteins.[5] Especially, the NMR resonances of the δ, ϵ, and ζ of Phe and the δ of Tyr tend to overlap each other, according to the NMR database (BioMagResBank URL: http://www.bmrb.wisc.edu/).[6] In addition, another difficulty lies in analyses of the aromatic resonances. Many measurement methods to assign them, using through-bond connectivity from the aliphatic resonances, have been reported.[7−11] However, an uncertain assignment method employing the NOE between aliphatic and aromatic resonances[12] is still generally used because some of the developed methods either are not sensitive enough or adopt the evolution of the poorly dispersed chemical shifts. The two problems described above have been factors that limit the application of NMR to structural determination because they become more serious as the molecular weight of the targeted protein increases.

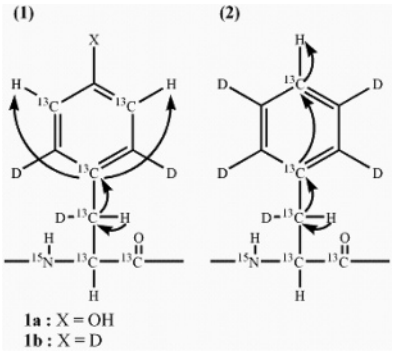

Figure 1. Stable isotope labeling patterns for Phe and Tyr, and magnetization transfer pathways for HBCBCGHE and HBCBCGCZHZ measurements. (1) $^{13}C_\gamma-^{13}C_\epsilon-^{1}H_\epsilon$ pattern for [$^{1}H_\beta-^{13}C_\beta-^{13}C_\gamma-^{13}C_\epsilon-^{1}H_\epsilon$]-Tyr (**1a**)/Phe (**1b**). (2) $^{13}C_\gamma-^{13}C_\zeta-^{1}H_\zeta$ pattern for [$^{1}H_\beta-^{13}C_\beta-^{13}C_\gamma-^{13}C_\zeta-^{1}H_\zeta$]-Phe (**2**). ^{12}C atoms are not shown in the figures. Arrows indicate the magnetization transfer pathways. In both cases, the transfer started from $^{1}H_\beta$.

To make the NMR spectra for aromatic resonances simple and sensitive, we developed a method to introduce novel ^{2}H, ^{13}C labeling patterns to Phe and Tyr and assignment strategies for the amino acids. As shown in Figure 1, one of the patterns is that all of the nonexchangeable hydrogens in the aromatic rings, except for the ϵ position, were replaced with ^{2}H, and the carbons at the γ and ϵ positions were labeled with ^{13}C, denoted

† CREST-JST.
‡ Graduate School of Science.

(1) Smith, B. O.; Ito, Y.; Raine, A.; Teichmann, S.; Ben-Tovim, L.; Nietlispach, D.; Broadhurst, R. W.; Terada, T.; Kelly, M.; Oschkimat, H.; Shibata, T.; Yokoyama, S.; Laue, E. D. *J. Biomol. NMR* **1996**, *8*, 360−368.
(2) Clore, G. M.; Starich, M. R.; Bewely, C. A.; Cai, M.; Kuszewski, J. *J. Am. Chem. Soc.* **1999**, *121*, 6513−6514.
(3) Aghazadeh, B.; Zhu, K.; Kubiseski, T. J.; Liu, G. A.; Pawson, T.; Zheng, Y.; Rosen, M. K. *Nat. Struct. Biol.* **1998**, *5*, 1098−1107.
(4) Medek, A.; Olejniczak, E. T.; Meadows, R. P.; Fesik, S. W. *J. Biomol. NMR* **2000**, *18*, 229−238.
(5) Yamazaki, T.; Yoshida, M.; Nagayama, K. *Biochemistry* **1993**, *32*, 5656−5669.
(6) Seavey, B. R.; Farr, E. A.; Westler, W. M.; Markley, J. L. *J. Biomol. NMR* **1991**, *1*, 217−236.
(7) Yamazaki, T.; Forman-Kay, J. D.; Kay, L. E. *J. Am. Chem. Soc.* **1993**, *115*, 11054−11055.
(8) Grzesiek, S.; Bax, A. *J. Am. Chem. Soc.* **1995**, *117*, 6527−6531.
(9) Carlomagno, T.; Maurer, M.; Sattler, M.; Schwendinger, M. G.; Glaser, S. J.; Griesinger, C. *J. Biomol. NMR* **1996**, *8*, 161−170.
(10) Lohr, F.; Ruterjans, H. *J. Magn. Reson. B* **1996**, *112*, 259−268.
(11) Prompers, J. J.; Groenewegen, A.; Hilbers, C. W.; Pepermans, H. A. M. *J. Magn. Reson.* **1998**, *130*, 68−75.
(12) Wüthrich, K. *NMR of Proteins and Nucleic Acids*; Wiley: New York, 1986.

10.1021/ja051386m CCC: $30.25

Scheme 1 [a]

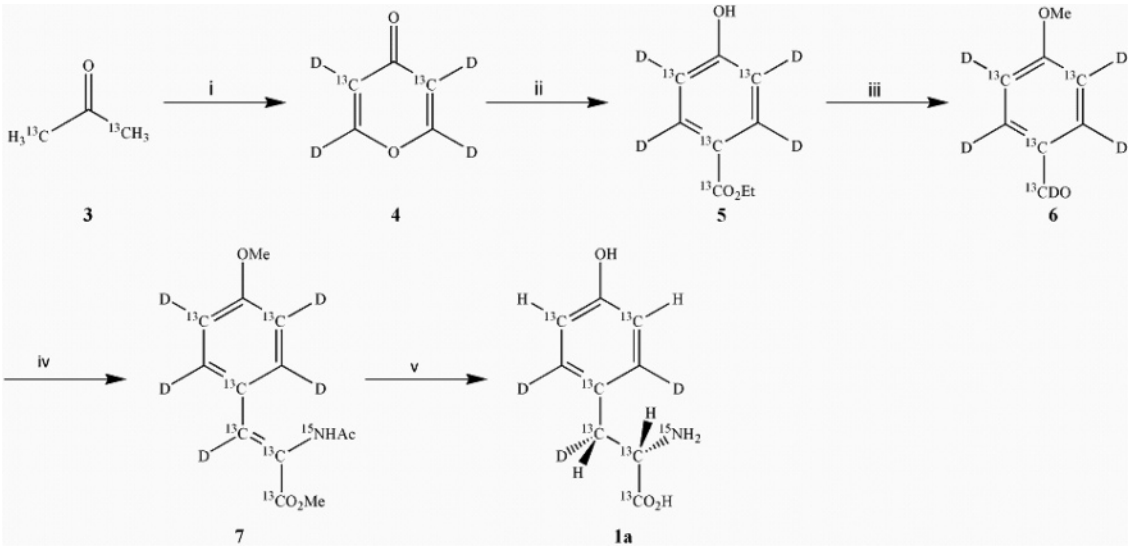

[a] Reagents and conditions: (i) (1) $(EtOCO)_2$, NaOEt, (2) conc DCl, (3) Cu; (ii) (1) [$^{13}C_3$]-ethyl malonate, *t*-BuOK/BuOD; (iii) (1) MeI, acetone, (2) $LiAlD_4$, (3) PDC; (iv) (1) [$^{13}C_2$;^{15}N]-NAc-glycine, Ac_2O, AcONa, (2) MeOH, Et_3N; (v) (1) (*S*,*S*)-Et-DuPhos-Rh, H_2, (2) 1N−HCl, (3) HBr−AcOH.

Scheme 2 [a]

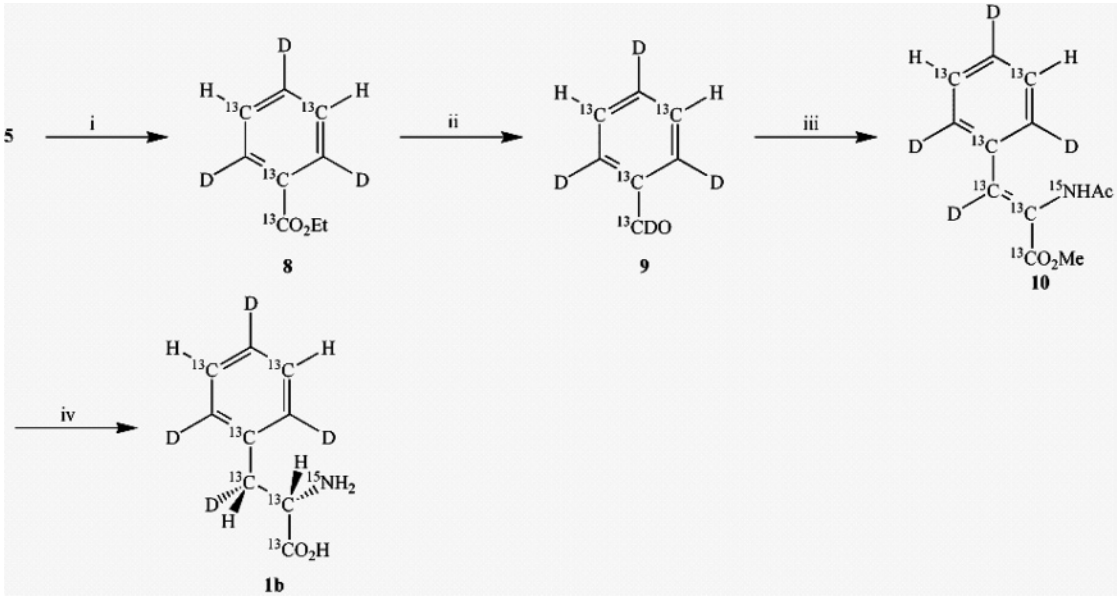

[a] Reagents and conditions: (i) (1) HCl, Δ, (2) Tet-Cl, K_2CO_3, (3) D_2, Pd/C; (ii) (1) $LiAlD_4$, (2) PDC; (iii) (1) [$^{13}C_2$;^{15}N]-NAc-glycine, Ac_2O, AcONa, (2) MeOH, Et_3N; (iv) (1) (*S*,*S*)-Et-DuPhos-Rh, H_2, (2) 1N−HCl.

as [$^{13}C_\gamma$−$^{13}C_\epsilon$−$^{1}H_\epsilon$]-Tyr (**1a**)/Phe (**1b**). The other is that the hydrogens at the δ and ϵ positions of Phe were replaced with ^{2}H, and the carbons at the γ and ζ positions were labeled with ^{13}C, denoted as [$^{13}C_\gamma$−$^{13}C_\zeta$−$^{1}H_\zeta$]-Phe (**2**), as shown in Figure 1. In both cases, the aliphatic moieties were uniformly labeled with ^{13}C and ^{15}N, and the *pro*-R proton of the β-methylene was stereospecifically labeled with ^{2}H, thus enabling the unambiguous chiral assignment for the prochiral methylene signals. Therefore, to use this novel isotope labeling strategy for NMR structure determinations of proteins, we chemically synthesized the labeled Phe and Tyr and then successfully incorporated these labeled amino acids into calmodulin, with a molecular weight of 17 kDa, by an *E. coli* cell-free system.[13−15] With the help of the extremely high protein yield of this cell-free system, as compared to in vivo expression systems,[15] only a few milligrams of the labeled amino acids were required to prepare the NMR samples. Here, the effectiveness of the samples is evaluated from the viewpoints of sensitivities and spectral overlap, and the assignment schemes are introduced.

We previously reported the stereoselective syntheses of Phe labeled with deuterium on the H_δ, H_ϵ, and H_ζ positions.[16] However, these synthetic routes were not suitable for the synthesis of these amino acids because of the difficulty in the regioselective incorporation of ^{13}C in the aromatic ring. In this work, the labeled amino acids described above were synthesized

(13) Torizawa, T.; Terauchi, T.; Kainosho, M. *Seikagaku* **2002**, *74*, 1279−1284.
(14) Torizawa, T.; Terauchi, T.; Kainosho, M. *Seibutsu Butsuri* **2004**, *44*, 200−205.
(15) Torizawa, T.; Shimizu, M.; Taoka, M.; Miyano, H.; Kainosho, M. *J. Biomol. NMR* **2004**, *30*, 311−325.
(16) Nishiyama, K.; Oba, M.; Ueno, R.; Morita, A.; Nakamura, Y.; Kainosho, M. *J. Labelled Compds.* **1994**, *9*, 831−837.

Scheme 3 [a]

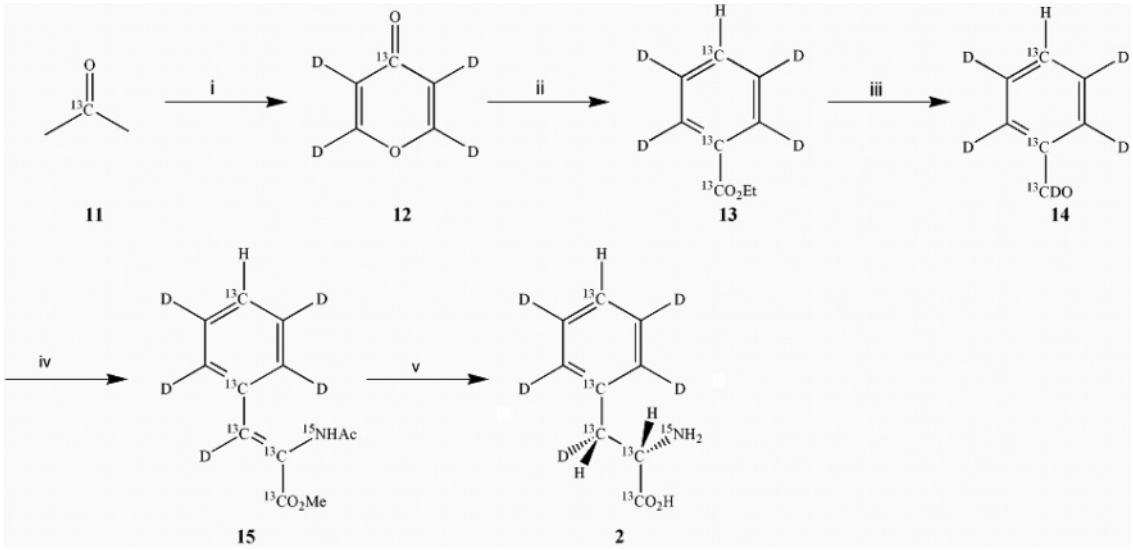

[a] Reagents and conditions: (i) (1) $(EtOCO)_2$, NaOEt, (2) conc DCl, (3) Cu; (ii) (1) [$^{13}C_3$]-ethyl malonate, *t*-BuOK/BuOD, (2) Tet-Cl, K_2CO_3, (3) H_2, Pd/C; (iii) (1) $LiAlD_4$, (2) PDC; (iv) (1) [$^{13}C_2$;^{15}N]-NAc-glycine, Ac_2O, AcONa, (2) MeOH, Et_3N; (v) (1) (*S*,*S*)-Et-DuPhos-Rh, H_2, (2) 1N−HCl.

efficiently, using a hydroxyl benzoic acid derivative as key intermediate, starting from various types of ^{13}C-labeled acetone and ethyl malonate.

From **3**, 4*H*-pyran-4-one **4** was obtained by a modification of reported procedure.[17,18] Then, 4*H*-pyran-4-one **4** was subjected to a condensation/aromatization reaction to give the key intermediate **5**.[19] For the synthesis of Tyr **1a** (Scheme 1), the hydroxyl group of **5** was methylated, and the ester was reduced by $LiAlD_4$. The following oxidation by PDC yielded **6**.[20] Then, **6** was converted into the dehydrotyrosine derivative **7** by a condensation with labeled Gly derivatives.[21,22] Compound **7** was subjected to hydrogenation in the presence of (*S*,*S*)-Et-DuPhos-Rh, as a catalyst in MeOH,[23] and then was deprotected to give Tyr **1a**.[24]

For the preparation of Phe **1b**, it is possible to synthesize it only by the deoxygenation of the hydroxyl group of the key intermediate **5**. Thus, a reductive deuteration of the hydroxyl group of **5** was carried out, using our recently reported methods to place a deuterium at the H_ζ position.[16,25] Then, as in the method for the synthesis of Tyr, **9** was converted into Phe **1b**.

For the synthesis of Phe **2** labeled simultaneously with ^{13}C in the ζ position and with deuterium in the δ and ϵ positions, [2-^{13}C]acetone was used instead of [1,3-$^{13}C_2$]acetone.

Experimental Section

Calmodulin was synthesized by the *E. coli* cell-free system, which we developed.[13−15] For the synthesis, the amounts of the labeled Phe and Tyr added were 1.32 and 0.37 mg, respectively. The [ul-^{13}C,^{15}N]-Phe and [ul-^{13}C,^{15}N]-Tyr were purchased from Cambridge Isotope Laboratories. Each unlabeled amino acid was added to the system to a final concentration of 1 mM. All of the NMR samples were prepared according to the previously published method.[15,26,27] Each NMR sample contained 0.5 mM calmodulin in 5 mM MES-d_{13} (Cambridge Isotope Laboratories), ca. 10 mM bis-Tris-d_{19} (Cambridge Isotope Laboratories) to adjust the pH to 6.5,[28] 5 mM $CaCl_2$, 0.1 mM NaN_3, and 10% D_2O or 100% D_2O. The NMR measurements were performed on a Bruker DRX600 spectrometer equipped with a CryoProbe at 37 °C.

The $^1H-^{13}C$ HSQC spectra[29] and the constant time (ct) version[30] for the aromatic resonances shown in Figure 2 were obtained using the samples in 100% D_2O. The other spectra were measured using the samples in 10% D_2O. The $^1H-^{13}C$ (ct) HSQC spectra shown in Figures 4 and 5 were acquired using coherence selection with sensitivity enhancement.[31−33] All of the HSQC measurements for aromatic resonances, except for the ct version, were performed under the following conditions: data size, 128 (t_1) × 1024 (t_2) complex points; $t_{1max}(^{13}C) = 30.3$ ms and $t_{2max}(^1H) = 128$ ms; and spectral widths in $\omega_1(^{13}C)$ and $\omega_2(^1H)$ of 4200 and 8000 Hz, respectively. The carrier frequencies of ^{13}C and ^1H were 126 and 4.7 ppm, respectively. In each t_1 increment, eight transients were accumulated, and the repetition delay was 1.2 s. The data set was zero-filled to 256 (t_1) × 2048 (t_2) complex points. The ct-HSQC spectrum for the aromatic resonances was obtained under the same conditions, except that the t_1 complex points were 70 and $t_{1max}(^{13}C) = 16.6$ ms, as limited by the constant evolution period of 17 ms. Compared to the ct-HSQC measurements for the aromatic resonances, the altered parameters in those for the aliphatic resonances were as follows: 256 (t_1) complex points, $t_{1max}(^{13}C) = 20.7$ ms, ct evolution = 26.6 ms, spectral width in ^{13}C = 12 000 Hz, carrier frequency of ^{13}C = 48 ppm, and zero-filling to 512 (t_1) complex points

(17) Riegel, E.; Zwilgmeyer, F. *Organic Syntheses*, Coll. Vol. II; Wiley: New York, 1943; p 126.
(18) *Organic Syntheses with Isotopes, Part II*; Interscience Publishers, Inc.: New York, 1958; p 1388.
(19) Lang, M.; Lang-Fugmann, S.; Steglich, W. *Organic Syntheses*; Wiley: New York, 2002; Coll. Vol. 78, pp 113−122.
(20) Beyer, J.; Lang-Fugmann, S.; Mühlbauer, A.; Steglich, W. *Synthesis* **1998**, 1047−1051.
(21) Erlenmeyer, E. *Justus Liebigs. Ann. Chem.* **1893**, *275*, 1−20.
(22) Ojima, I.; Kato, K.; Fujita, M. *J. Org. Chem.* **1989**, *54*, 4511−4522.
(23) Burk, M.; Feaster, J.; Nugent, W.; Harlow, R. *J. Am. Chem. Soc.* **1993**, *115*, 10125−10138.
(24) Li, G.; Patel, D.; Hurby, V. *Tetrahedron Lett.* **1993**, *34*, 5393−5396.
(25) Viswanatha, V.; Hruby, V. J. *J. Org. Chem.* **1980**, *45*, 2010−2012.
(26) Ikura, M.; Marion, D.; Kay, L. E.; Shih, H.; Krinks, M.; Klee, C. B.; Bax, A. *Biochem. Pharmacol.* **1990**, *40*, 153−160.
(27) Ikura, M.; Kay, L. E.; Bax, A. *Biochemistry* **1990**, *29*, 4659−4667.
(28) Kelly, A. E.; Ou, H. D.; Withers, R.; Dotsch, V. *J. Am. Chem. Soc.* **2002**, *124*, 12013−12019.
(29) Bodenhausen, G.; Ruben, D. J. *Chem. Phys. Lett.* **1980**, *69*, 185−189.
(30) Vuister, G. W.; Bax, A. *J. Magn. Reson.* **1998**, *98*, 428−435.
(31) Palmer, A. G., III; Cavanagh, J.; Wright, P. E.; Rance, M. *J. Magn. Reson.* **1991**, *93*, 151−170.
(32) Kay, L. E.; Keifer, P.; Saarinen, T. *J. Am. Chem. Soc.* **1992**, *114*, 10663−10665.
(33) Schleucher, J.; Schwendinger, M.; Sattler, M.; Schmidt, P.; Schedletzky, O.; Glaser, S. J.; Sorensen, O. W.; Griesinger, C. *J. Biomol. NMR* **1994**, *4*, 301−306.

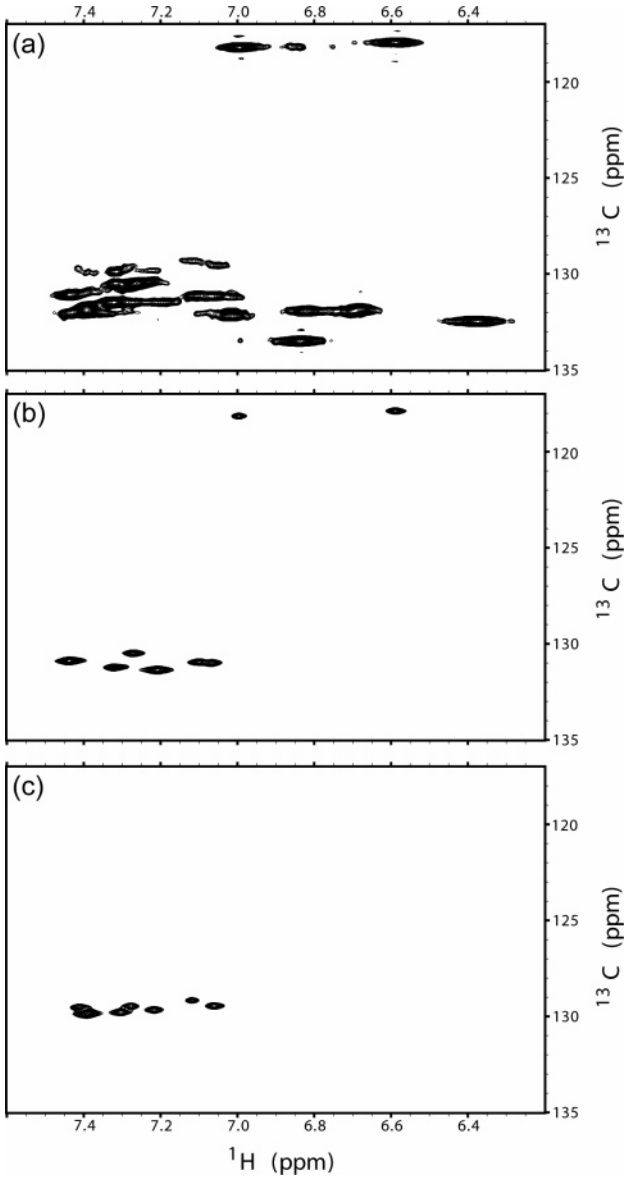

Figure 2. ^{1}H−^{13}C correlated spectra of calmodulin. (a) ct-HSQC spectrum of [ul-^{13}C,^{15}N]-Phe and -Tyr selectively labeled calmodulin. (b) HSQC spectrum of [$^{13}C_{\gamma}$−$^{13}C_{\epsilon}$−$^{1}H_{\epsilon}$]-Tyr (**1a**) and Phe (**1b**) selectively labeled calmodulin. (c) HSQC spectrum of [$^{13}C_{\gamma}$−$^{13}C_{\zeta}$−$^{1}H_{\zeta}$]-Phe (**2**) selectively labeled calmodulin. In (a), the ^{13}C region between 130 and 135 ppm contains the resonances of the δ, ϵ, and ζ of Phe, and the δ of Tyr. The corresponding regions in (b) and (c) contain only the resonances of ϵ and ζ of Phe, respectively. In another region near 118 ppm in (a) and (b), the ϵ resonances of Tyr are detected. The small chemical shift differences between (a) and (b) or (a) and (c) are caused by isotope shifts.

prior to transformation. During the ct evolution, ^{2}H continuous wave decoupling was applied with a field strength of 0.72 kHz. For the 3D HBCB(CG)HE measurement, the acquisition parameters were set as follows: data size, 16 (t_1) × 16 (t_2) × 512 (t_3) complex points; $t_{1max}(^{1}H_{\beta}) = 13.3$ ms, $t_{2max}(^{13}C_{\beta}) = 8.8$ ms and $t_{3max}(^{1}H_{\epsilon}) = 64$ ms; and spectral widths in ω_1 ($^{1}H_{\beta}$), ω_2 ($^{13}C_{\beta}$), and ω_3 ($^{1}H_{\epsilon}$) of 1200, 1800, and 8000 Hz, respectively. The eight scans per increment and the 1 s repetition delay gave a measuring time of 3.4 h. The data set was zero-filled to 32 (t_1) × 32 (t_2) × 1024 (t_3) complex points. For the 2D (HB)CB(CG)HE measurement, the parameters for the 3D measurement were used by reducing the dimension. The 32 scans per increment resulted in a measuring time of 25 min. The 3D HBCB(CGCZ)HZ spectrum was obtained under the same conditions as the 3D HBCB(CG)HE measurement, except for the differences of t_2 complex points = 8, $t_{2max}(^{13}C_{\beta}) = 8.8$ ms, spectral width in ^{13}C = 9000 Hz, number of scans per increment = 16 and zero-filling to 16 (t_2) complex points prior to transformation. The total measurement time of the 3D spectrum was 3.4 h. Prior to Fourier transformation, the data matrices were multiplied with a 60° -shifted sine bell window in the indirect dimensions and a 45°-shifted sine bell window in the acquisition dimension.[34] Data processing was performed with the program XWIN-NMR, version 3.5 (Bruker), and for the data analysis, the program SPARKY, version 3.106 (Goddard and Kneller, University of California, San Francisco), was used. The ^{1}H chemical shifts were referenced to external DSS, and the ^{13}C and ^{15}N shifts were indirectly referenced.[35,36]

Results and Discussion

We compared the ^{1}H−^{13}C HSQC spectra of calmodulin samples labeled according to the patterns in Figure 1 (Figure 2b) using a constant time (ct) version of the measurement of the protein, in which the Phe and Tyr residues were uniformly ^{13}C-labeled (Figure 2a). As a result, the signal overlapping was alleviated in Figure 2b, due to the disappearance of some resonances and the sharpening of the residual resonances. Sensitivity improvements were also observed (averaged ratios of the signal intensities to those of the uniformly ^{13}C-labeled rings: Phe ϵ: 13, ζ: 26, Tyr: 4). One of the reasons for the improvement is the attenuation of the dipolar interactions, by replacing the hydrogens adjacent to the detecting nuclei with ^{2}H. In the case of the uniformly ^{13}C-labeled aromatic residues, a long ct (∼17 or 34 ms) evolution period, which causes a reduction of the magnetization, must be used in the ^{1}H−^{13}C HSQC measurement so that the ^{13}C−^{13}C coupling can be refocused. On the other hand, the novel labeling patterns do not require the constant time evolution in the measurement. This is another reason the spectra had improved sensitivity. TROSY in a ct evolution manner has been developed for the sensitive detection of aromatic resonances in uniformly ^{13}C-labeled proteins.[37] By altering the evolution period to remove the constant time, this measurement technique would allow more sensitive detection of the aromatic resonances of the novel labeling patterns in larger proteins.

The schemes for the assignments of the aromatic resonances are shown in Figure 3. The pathways of magnetization are as follows:

(a) HBCB(CG)HE (H_{β} (t_1) → C_{β} (t_2) → C_{γ} → H_{ϵ} (t_3))

(b) HBCB(CGCZ)HZ (H_{β} (t_1) → C_{β} (t_2) → C_{γ} → C_{ζ} → H_{ζ} (t_3))

These pulse sequences were composed of previously summarized building blocks.[38] The most similar pulse sequence is either $(H_{\beta})C_{\beta}(C_{\gamma}C_{\delta})$ H_{δ} or $(H_{\beta})C_{\beta}(C_{\gamma}C_{\delta}C_{\epsilon})H\epsilon$, previously reported by Yamazaki et al.[7] One of the major differences between the previously published sequences and our sequences is the incorporation of H_{β} evolution. The overlap of the H_{β} resonances is alleviated, and the relaxation time of the evolving H_{β} is prolonged, due to the stereoselective deuteration in the

(34) DeMacro, A.; Wuthrich, K. *J. Magn. Reson.* **1976**, *24*, 201−204.
(35) Wishart, D. S.; Bigam, C. G.; Yao, J.; Abildgaard, F.; Dyson, H. J.; Oldfield, E.; Markley, J. L.; Sykes, B. D. *J. Biomol. NMR* **1995**, *6*, 135−140.
(36) Markley, J. L.; Bax, A.; Arata, Y.; Hilbers, C. W.; Kaptein, R.; Sykes, B. D.; Wright, P. E.; Wuthrich, K. *Eur. J. Biochem.* **1998**, *256*, 1−15.
(37) Pervushin, K.; Riek, R.; Wider, G.; Wuthrich, K. *J. Am. Chem. Soc.* **1998**, *120*, 6394−6400.
(38) Edison, A. S.; Abildgaard, F.; Westler, W. M.; Mooberry, E. S.; Markley, J. L. *Methods Enzymol.* **1994**, *239*, 3−79.

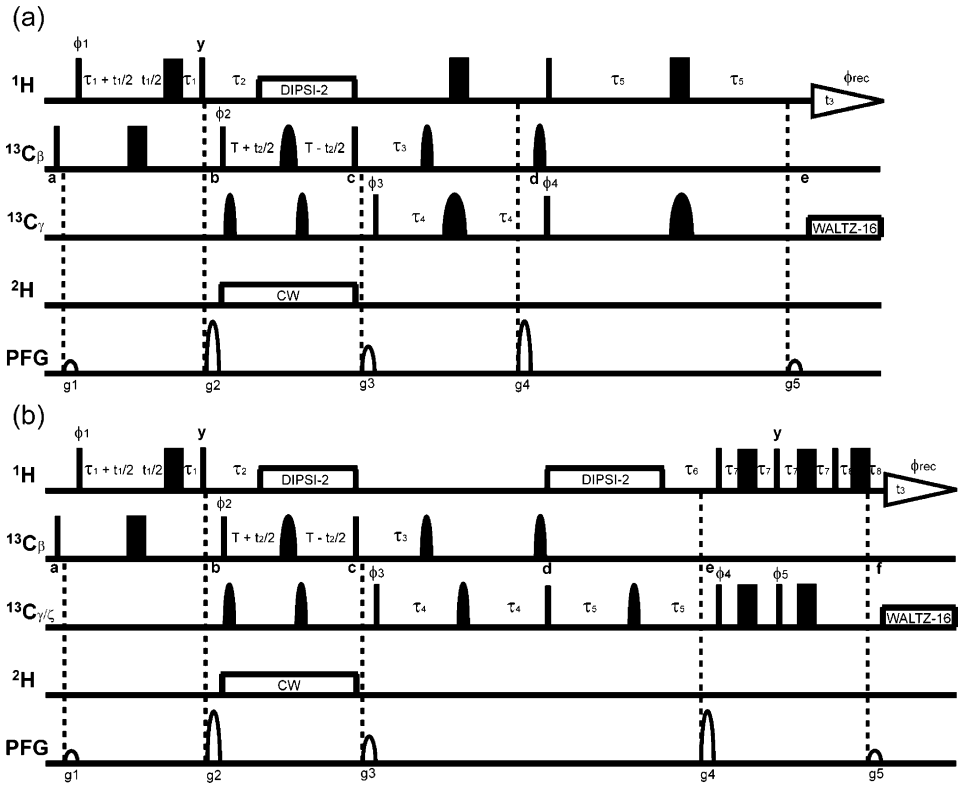

Figure 3. Pulse sequences of the (a) HBCB(CG)HE and (b) HBCB(CGCZ)HZ measurements. In both pulse sequences, the radio frequency (rf) pulses on ^{1}H between points a and b, ^{1}H between b and acquisition, and ^{2}H were applied at 3, 4.7, and 2.5 ppm, respectively. In (a), the carrier frequency of $^{13}C_\beta$ was set to 39 ppm, and that of $^{13}C_\gamma$ was set to 137 ppm for Phe or to 129 ppm for Tyr. In (b), the rf pulses on $^{13}C_\beta$ and $^{13}C_{\gamma/\zeta}$ were irradiated at 38 and 134 ppm. Narrow and wide black bars indicate nonselective 90 and 180°, respectively. Sine bell shapes on the lines marked with $^{13}C_\gamma$ and $^{13}C_{\gamma/\zeta}$ indicate selective 180° pulses at the corresponding frequencies with a *g*3 shape.[40] The pulses were applied along *x* if no phase is marked above the pulses. All ^{1}H pulses were applied with a 20 kHz field, while the ^{1}H DIPSI-2 decoupling[41] employed a 5 kHz field. All of the rectangular ^{13}C 90 and 180° pulses were applied with 37 and 18.5 kHz fields, respectively. The first selective $^{13}C_\beta$ 180° pulses were applied with a duration of 1.2 ms. Selective 180° pulses with a duration of 600 μs were used for the second and third pulses on $^{13}C_\beta$ and for the first and second pulses on $^{13}C_\gamma/^{13}C_{\gamma/\zeta}$. The third and fourth selective 180° pulses for $^{13}C_\gamma/^{13}C_{\gamma/\zeta}$ were applied with durations of 2.2 ms in (a) and 600 μs in (b). ^{13}C decoupling during acquisition was achieved using 2 kHz WATLZ-16 decoupling.[42] For ^{2}H decoupling, continuous wave irradiation was accomplished with a field strength of 0.72 kHz during the blocks between points b and c (denoted as CW in the sequences). Pulsed-field gradients were applied along the *z*-axis with a sine bell shape and with a duration of 1 ms. Amplitudes of the gradients are as follows: $g1 = 5$ G/cm, $g2 = 40$ G/cm, $g3 = 15$ G/cm, $g4 = 40$ G/cm, $g5 = 10.1$ G/cm. The first gradient (*g*1) was applied to ensure that the magnetization giving rise to the signal originates on ^{1}H, and not ^{13}C.[43] The second and third gradients (*g*2 and *g*3) were used for a heteronuclear *zz*-filter.[44] The fourth and fifth gradients (*g*4 an *g*5) were applied for coherence pathway selection.[33] The delays commonly used in (a) and (b) were $\tau_1 = 1.8$ ms, $\tau_2 = 3.7$ ms, $\tau_3 = 5.2$ ms, and $T = 5.2$ ms. The delays in (a) were $\tau_4 = 7.2$ ms and $\tau_5 = 12$ ms, and in (b), $\tau_4 = 6$ ms, $\tau_5 = 6$ ms, $\tau_6 = 3.1$ ms, $\tau_7 = 1.5$ ms, and $\tau_8 = 1.2$ ms. The phases were cycled as: $\phi1 = \{x, -x\}$; $\phi2 = \{x\}$; $\phi3 = \{4x, -4x\}$; $\phi4 = \{2x, -2x\}$; $\phi5 = \{-2y, 2y\}$; $\phi_{rec} = \{x, -2x, x, -x, 2x, -x\}$. Quadrature detections in the t_1 and t_2 dimensions were obtained by altering the phases $\phi1$ and $\phi2$ according to the States-TPPI manner,[39] respectively.

β-methylene group. These are the reasons why our pulse sequences include the H_β evolution. In addition, the slower relaxation of $^{13}C_\beta$, due to the deuteration, also enhances the measurement sensitivity. In the meantime, ^{2}H decoupling must be applied during the ^{13}C evolution time to avoid splitting by the $^{13}C-^2H$ coupling. In the case of HBCB(CG)HE, the magnetization is transferred from C_γ to detect H_ϵ directly via $^3J_{C_\gamma H_\epsilon}$ (7.9 Hz for Phe, 7.1 Hz for Tyr), after the transfer to C_γ. On the other hand, HBCB(CGCZ)HZ transfers the magnetization from C_γ to C_ζ via $^3J_{C_\gamma C_\zeta}$ (9.3 Hz), before the last $C_\zeta-H_\zeta$ one-bond INEPT transfer. The site-specific ^{2}H- and ^{13}C-labeling patterns made it possible to transfer the magnetizations through the long-range couplings. One should optimize the delays for magnetization transfer using such small *J* couplings by considering the relaxation times. Here, we determined the values so that the intensities of the correlations could be maximized in the calmodulin spectra. Figures 4 and 5 illustrate the spectra for the H_ϵ/C_ϵ assignments of Phe and Tyr, and for the H_ζ/C_ζ assignments of Phe, respectively. The averaged C_γ chemical shifts of Phe and Tyr are separated well (136.78 and 128.97 ppm, respectively, obtained from BioMagResBank). Therefore, the HBCB(CG)HE correlations of Phe and Tyr could be detected individually by setting the frequencies to the individual averaged shifts, as shown in Figure 4b,c,f. Calmodulin has eight Phe (12, 16, 19, 65, 68, 89, 92, and 141) and two Tyr (99 and 138) residues. In Figure 4, all of the correlations of the Phe and Tyr residues could be detected. For the assignment of the H_ϵ/C_ϵ of Phe, the 3D spectrum was measured (~3.4 h). However, the reduced dimensional 2D spectrum, like the spectrum shown in Figure 4f for Tyr, would be sufficient even for the assignment of Phe. Yamazaki et al. measured the 2D $(H_\beta)C_\beta(C_\gamma C_\delta C_\epsilon)H\epsilon$ spectrum of a 104 residue protein complexed with a 12 residue peptide at 30 °C on a 500 MHz spectrometer, resulting in a measurement time of 20 h.[7] Compared to this previous method, our labeling pattern and the 2D measurement (with the assistance of a cryogenic probe) could reduce the time needed to detect the correlations between β and ϵ to 25 min.

Figure 5 also shows all of the correlations of HBCB(CGCZ)-HZ of Phe. The 3D measurement had a sensitivity similar to that of 3D HBCB(CG)HE (~3.4 h). The H_ζ/C_ζ assignments of Phe would also be performed easily, even if the 2D version is measured, as inferred from the 2D projections shown in Figure

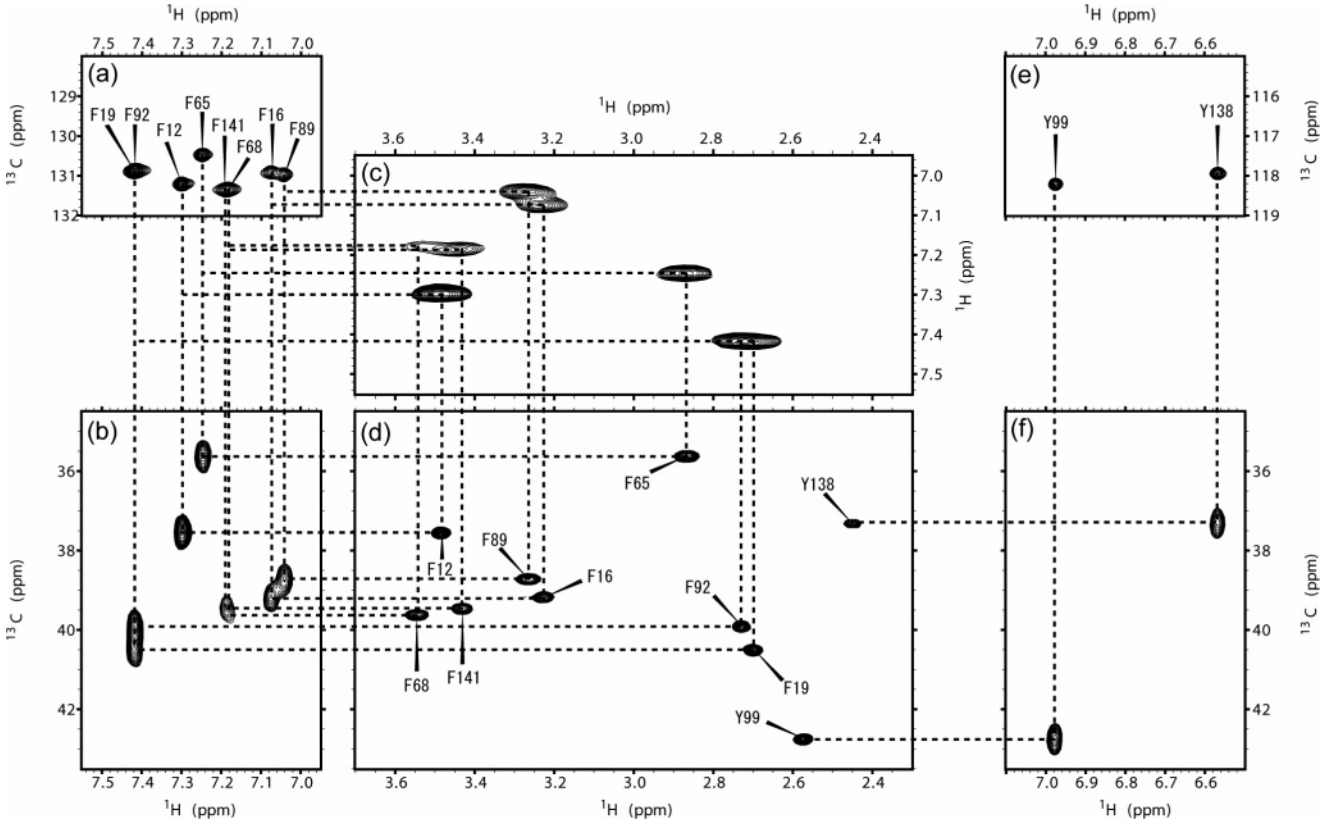

Figure 4. Connection between H_ϵ/C_ϵ and H_β/C_β of Phe and Tyr using the 3D or 2D HBCB(CG)HE spectrum of [$^{13}C_\gamma-^{13}C_\epsilon-^1H_\epsilon$]-Phe and -Tyr selectively labeled calmodulin. (a) $^1H-^{13}C$ HSQC spectrum for aromatic resonances (Phe-H_ϵ/C_ϵ region). (b) 2D $C_\beta-H_\epsilon$ projection of the 3D HBCB(CG)HE spectrum for Phe. (c) 2D $H_\beta-H_\epsilon$ projection of the 3D HBCB(CG)HE spectrum for Phe. (d) $^1H-^{13}C$ ct-HSQC spectrum for aliphatic resonances (Phe and Tyr-H_β/C_β region). (e) $^1H-^{13}C$ HSQC spectrum for aromatic resonances (Tyr-H_ϵ/C_ϵ region). (f) 2D (HB)CB(CG)HE spectrum for Tyr. Assignments are indicated alongside the corresponding signals with the one-letter amino acid code and the residue number. Aromatic and aliphatic resonances are connected with dotted lines through the HBCB(CG)HE spectra.

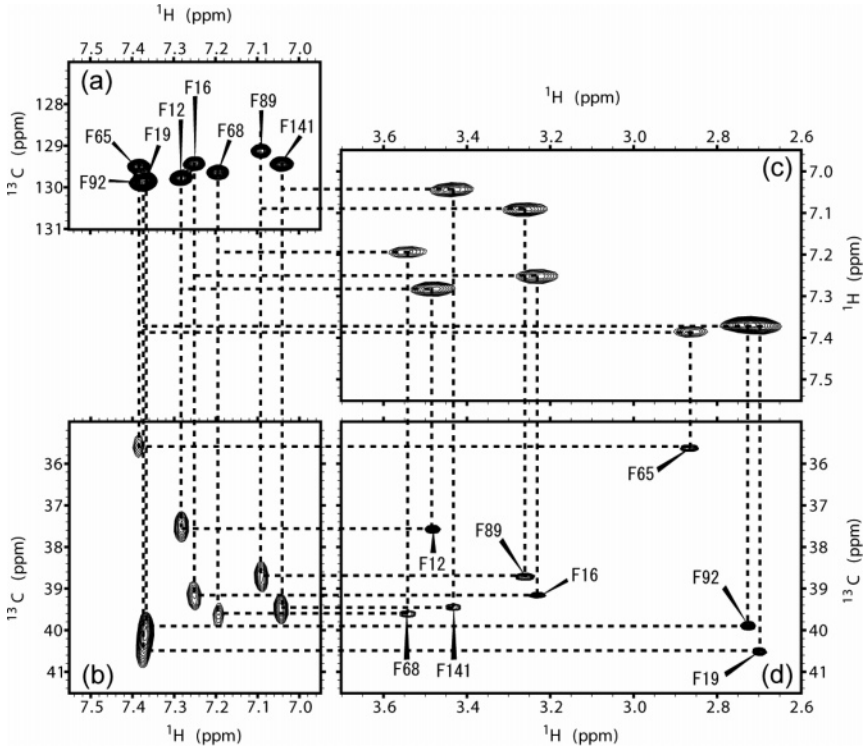

Figure 5. Connection between H_ζ/C_ζ and H_β/C_β of Phe using the 3D HBCB(CGCZ)HZ spectrum of [$^{13}C_\gamma-^{13}C_\zeta-^1H_\zeta$]-Phe, selectively labeled calmodulin. (a) $^1H-^{13}C$ HSQC spectrum for aromatic resonances. (b) 2D $C_\beta-H_\zeta$ projection of the 3D HBCB(CGCZ)HZ spectrum. (c) 2D $H_\beta-H_\zeta$ projection of the 3D HBCB(CGCZ)HZ spectrum. (d) $^1H-^{13}C$ ct-HSQC spectrum for aliphatic resonances (H_β/C_β region).

5. In the measurements of both HBCB(CG)HE and HBCB(CGCZ)HZ, we utilized the relatively well separated H_β, C_β, and H_ϵ/H_ζ chemical shifts. However, if necessary, C_γ evolution in HBCBCGHE can easily be introduced to the pulse scheme, by modifying the building block between points c and d, to contain the evolution time, and by altering ϕ_3, the receiver phases, and g4 to exploit the echo/anti-echo manner for quadrature detection.[31] In the same way, the building block between points c and d, which includes an evolution period, and the alteration of ϕ_3 for the States-TPPI quadrature detection manner[39] are necessary for C_γ evolution in HBCBCGCZHZ, and the block between points d and e for evolution and the alteration of ϕ_5 and g4 for the echo/anti-echo manner are required for C_ζ evolution.

Conclusions

We have proposed novel stable isotope labeling patterns for Phe and Tyr in proteins. The NMR samples of calmodulin, in which the amino acids were introduced, were successfully prepared by chemical synthesis of the amino acids and protein production with the *E. coli* cell-free system. The labeling patterns diminished the spectral overlap and allowed sensitive detection. The straightforward pulse schemes developed for the labeling patterns also afforded sensitive spectra. The unambiguously assigned aromatic resonances are expected to be useful for the structural determinations of proteins, as will be described elsewhere.

Acknowledgment. We thank Prof. Mitsuhiko Ikura of Toronto University for providing the calmodulin gene. This work was supported by CREST/JST.

JA051386M

(39) Marion, D.; Ikura, M.; Tschudin, R.; Bax, A. *J. Magn. Reson.* **1989**, *85*, 393.
(40) Emsley, L.; Bodenhausen, G. *Chem. Phys. Lett.* **1987**, *165*, 469.
(41) Shaka, A. J.; Lee, C. J.; Pines, A. *J. Magn. Reson.* **1988**, *77*, 274−293.
(42) Shaka, A. J.; Keeler, J.; Frenkiel, T.; Freeman, R. *J. Magn. Reson.* **1993**, *52*, 335.
(43) Kay, L. E. *J. Am. Chem. Soc.* **1993**, *115*, 2055−2057.
(44) Montelione, G. T.; Lyons, B. A.; Emerson, S. D.; Tashiro, M. *J. Am. Chem. Soc.* **1992**, *114*, 10974−10975.